AIP | Applied Physics Letters

An ultrafast nanotip electron gun triggered by grating-coupled surface plasmons

Benjamin Schröder, Murat Sivis, Reiner Bormann, Sascha Schäfer, and Claus Ropers

Citation: Applied Physics Letters **107**, 231105 (2015); doi: 10.1063/1.4937121
View online: http://dx.doi.org/10.1063/1.4937121
View Table of Contents: http://scitation.aip.org/content/aip/journal/apl/107/23?ver=pdfcov
Published by the AIP Publishing

An ultrafast nanotip electron gun triggered by grating-coupled surface plasmons

Benjamin Schröder, Murat Sivis, Reiner Bormann, Sascha Schäfer, and Claus Ropers[a)]
4th Physical Institute - Solids and Nanostructures, University of Göttingen, Friedrich-Hund-Platz 1, 37077 Göttingen, Germany

(Received 17 September 2015; accepted 23 November 2015; published online 9 December 2015)

We demonstrate multiphoton photoelectron emission from gold nanotips induced by nanofocusing surface plasmons, resonantly excited on the tip shaft by a grating coupler. The tip is integrated into an electron gun assembly, which facilitates control over the spatial emission sites and allows us to disentangle direct grating emission from plasmon-triggered apex emission. The nanoscale source size of this electron gun concept enables highly coherent electron pulses with applications in ultrafast electron imaging and diffraction. © *2015 AIP Publishing LLC*.
[http://dx.doi.org/10.1063/1.4937121]

The field of plasmonics has established a wide range of approaches to cast a free electron gas in designed geometries for a controlled collection, guiding, and concentration of light on the nanoscale.[1–5] As a prominent example, nanofocusing harnesses both the waveguiding and sub-wavelength localization capabilities of plasmonic excitations, by converging propagating surface plasmon polaritons (SPPs) on tapered conical structures in an intense near-field at the cone apex.[6–20] This optical hot spot locally drives multiple linear and nonlinear processes,[10–13] which have given rise to applications in near-field scanning optical microscopy (NSOM) and spectroscopy.[14–20] Grating-coupling has proven as a very efficient means to launch surface plasmons on metal nanotips,[10] and it allows for a spatial separation of the in-coupling location from the plasmonic focus. Initially designed to reduce background signals in NSOM and to avoid direct sample excitation, the scheme is particularly suited for inducing highly nonlinear optical processes, such as multiphoton photoemission.[21,22] Localized photoelectron emission from a nanoscale apex[21–35] is of great importance for future developments in the field of time-resolved electron imaging and diffraction.[36–44] First applications have utilized the unique beam properties of tip-based photoelectron sources[45,46] in ultrafast transmission electron microscopy (UTEM),[47] ultrafast low-energy electron diffraction (ULEED),[48] and femtosecond point-projection microscopy (fs-PPM)[49,50] with a recent PPM implementation based on plasmonic nanofocusing.[51] Whereas lens-less imaging approaches make use of nanoscale source sizes, the full capabilities of coherent electron pulses, including nanoscale probing and phase contrast imaging, can be most efficiently harnessed in a UTEM setting. Thus, it is highly desirable to combine a plasmonic nanofocusing source with a gun environment compatible with electron microscopy.

Here, we demonstrate multiphoton photoemission from the apex of a gold nanotip driven by resonant femtosecond excitation of surface plasmons in a grating coupler on the tip shaft. The emitter is integrated in a modified field emission gun allowing for a detailed characterization and control of the active emission sites. In this setup, by tailoring the electrostatic field around the tip, electron emission from the apex, grating, and shaft can be clearly distinguished. The ultrafast electron source developed here will be applicable in a variety of time-resolved electron imaging approaches.

In the experiments (schematic of the setup shown in Fig. 1), optical excitation is provided by a mode-locked Ti:Sapphire laser oscillator (center wavelength 800 nm, pulse duration 10 fs, and repetition rate 78 MHz). The laser beam is focused onto the gold nanotip (spot diameter of 12 μm) by a plano-convex lens mounted on a three-dimensional translation stage. The power and polarization of the laser beam are controlled by a $\lambda/2$-waveplate and a broadband polarizer. Sharp gold tips are fabricated by electrochemical etching of thermally annealed gold wires (0.25 mm diameter) in hydrochloric acid (for a detailed description of the fabrication process, see, e.g., Refs. 14 and 19). To facilitate an efficient SPP excitation, a resonant grating structure is milled into the shaft by focused ion beam etching. The grating is placed 45 μm from the apex, allowing for a separate excitation of both regions. Figure 2(a) displays a scanning electron micrograph of one of the measured gold tips with an apex radius of curvature of 22 nm and a grating periodicity of 800 nm. The nanostructured tip is built into a field emission gun comprising a suppressor and extractor unit installed in an ultra-high vacuum chamber (operating pressure in the 10^{-9} mbar range). Distributions of emitted electrons are recorded by an imaging microchannel plate (MCP) detector and a charge-coupled device (CCD) camera.

We have observed grating-induced multiphoton photoemission from multiple nanostructured tips. Both the high nonlinearity of the emission (a four-photon process is expected from the excitation wavelength and the gold work function[21]) as well as the polarization dependence of the grating coupler are evident from a measurement of the photocurrent as a function of waveplate angle $\alpha/2$ (Fig. 1(d)). We find maximum emission for p-polarization (electric field perpendicular to grooves), in agreement with recent observations,[51] and the shape of the polar plot exhibits an effective nonlinearity in intensity of $n = 3.4$ (red line corresponds to a $\cos^{2n}(\alpha + \phi)$ dependence with $\phi = 4°$). A more direct

a)cropers@gwdg.de

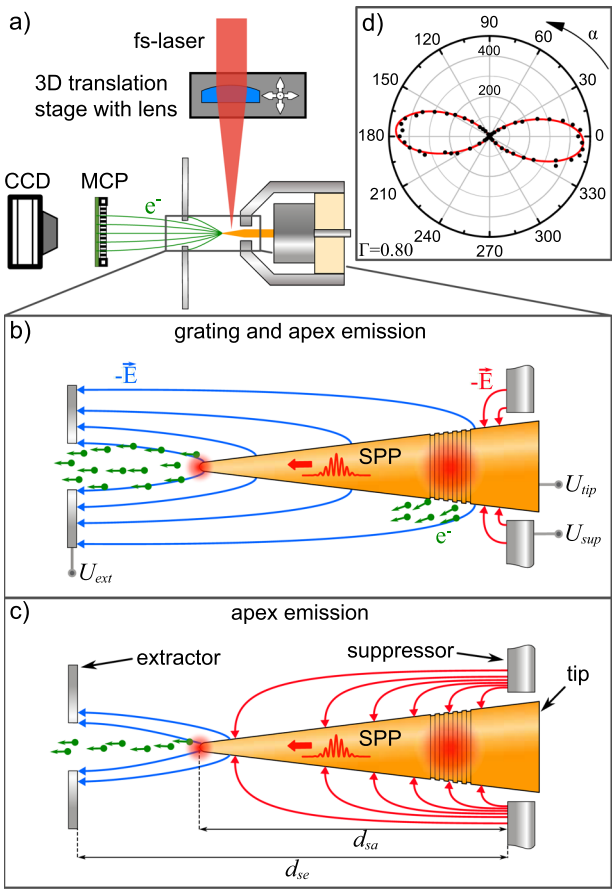

FIG. 1. Schematic of the experimental setup. (a) The excitation laser is focused onto the nanostructure by a plano-convex lens (focal length: 100 mm) mounted on a translation stage. Emitted electrons are detected by an MCP and CCD camera. The gold tip is inserted into a suppressor-extractor-geometry allowing for separate tuning of the static potentials of the tip (U_{tip}), suppressor (U_{sup}), and extractor (U_{ext}) electrodes. (b) Schematic field line distribution for a voltage setting resulting in electron extraction from the entire tip (blue lines). (c) A more negative suppression voltage prevents emission (red lines) from the grating and shaft. Any electron emission observed under these conditions, e.g., upon grating excitation, must stem from regions close to the apex. (d) Electron rate (s^{-1}) as a function of polarization angle α upon grating illumination (average power: 14.5 mW, waveplate is rotated between 0° and 180°). (d_{se} = 1.44 mm and d_{sa} = 0.29 mm, distance between MCP and tip apex: 36 mm, MCP diameter: 26 mm, and extractor aperture diameter: 3 mm)

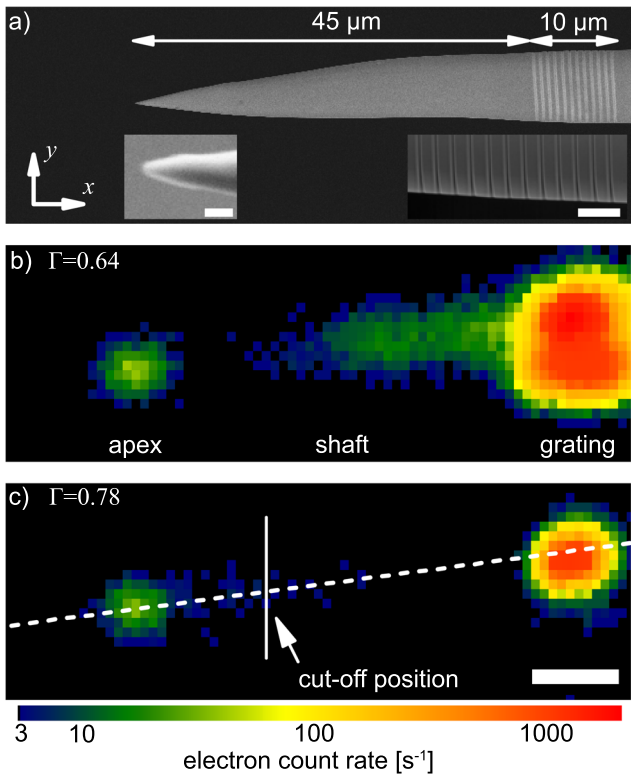

FIG. 2. (a) Scanning electron micrograph of the tip including the nanofabricated grating (12 grooves, 200 nm width, and 500 nm depth). Insets: (left) apex region (scale bar: 100 nm), (right) closeup of the grating region (scale bar: 2 μm). (b) and (c) Color-coded maps of the detected electron count rate (logarithmic scale) as a function of the focal position in the *xy*-plane, obtained by raster scanning the lens (polarization parallel to tip axis (α = 0), average laser power: 17 mW). (b) A suppressor voltage of $U_{sup} = -460$ V ($\Gamma = 0.64$) allows for electron emission from the apex, shaft and grating regions (compare Fig. 1(b)). (c) A more negative suppression voltage ($U_{sup} = -475$ V, $\Gamma = 0.78$) leads to a cut-off position between the apex and grating, as indicated by the white vertical line. The measurement shown in Fig. 3(b) is recorded along the white dashed line in (c). Scale bar: 10 μm. Throughout all measurements, the tip and extractor voltages are kept constant at $U_{tip} = -400$ V and $U_{ext} = 0$ V, respectively.

measurement of the effective nonlinearity of the emission process will be presented below.

Recording electron emission patterns yields information about the total current generated by optical excitation at the focal position. The present structure is designed to produce electron emission in the apex region, which is substantially removed from the optical excitation position at the grating. In order to distinguish direct photoemission at the focal position from plasmon-mediated emission, we manipulate the electrostatic environment of the field emitter geometry. As we will demonstrate, this allows for the suppression of emission directly from the grating while retaining apex emission induced by grating-coupled surface plasmons.

Specifically, for given tip (U_{tip}) and extractor (U_{ext}) voltages, the suppressor voltage (U_{sup}) defines a point along the tip axis, at which the electric field changes its sign. On the left side (towards the apex) of this field-reversal point or cut-off position, electrons are effectively extracted, whereas emission is suppressed towards the shaft (compare Figs. 1(b) and 1(c)). By variation of the suppressor voltage, the field-reversal point can be continuously shifted across the grating and shaft. Note that the static extraction fields always remained below the onset of field emission (finite element simulations yielded fields of 0.1–0.4 V/nm).

Figures 2(b) and 2(c) show color-coded maps of the electron count rate as a function of the laser focus position in the *xy*-plane (same area as shown in Fig. 2(a)), obtained by raster scanning the lens position. Here, Fig. 2(c) corresponds to a voltage setting with suppression of direct emission from the grating (cut-off point between apex and grating), whereas grating emission is permitted in Fig. 2(b) (cut-off point on the right of the grating). In both measurements, two clear positions of enhanced electron count rates are recorded, corresponding to an excitation either on the apex or on the grating. Illumination on smooth parts of the shaft results in smaller rates with a Γ-dependent spatial distribution.

The precise location of the field-reversal point is identified by measuring line scans in the *xy*-plane (dashed line in Fig. 2(c)) for a range of suppressor voltages, as demonstrated in Fig. 3. In this figure, the variation of the suppressor

voltage (vertical scale) is represented by using a dimensionless parameter Γ, defined as[52]

$$\Gamma = \frac{(U_{tip} - U_{sup})}{(U_{ext} - U_{sup})} \frac{d_{se}}{d_{sa}}. \quad (1)$$

Here, d_{sa} and d_{se} are the distances from the apex and extractor to the suppressor, respectively (cf. Fig. 1(c)). Complete suppression of photoelectrons from the tip is given for a Γ value on the order of unity (field reversal point crosses the apex) with a precise value depending on the specific geometry. For decreasing Γ, the field cut-off is shifted from the apex towards the suppressor, widening the region where photoelectrons can be extracted. Figure 3(b) shows a Γ-dependent map of line scans exhibiting various features, which are assigned to particular emission regions in the schematic shown in Fig. 3(a). The photoemission map reveals three prominent contributions: Two vertical lines with the excitation positioned at the apex and the grating, respectively, and a diagonal stripe extending throughout the shaft and grating regions. The signal from direct apex excitation is nearly constant as a function of Γ. For $\Gamma_a = 0.83$, the field-reversal point reaches the apex position ($x = 0$) and suppresses the emission. Consistently, a linear trend of the upper edge of the diagonal shaft feature is observed: It marks the Γ-dependent shift of the cut-off position $x_{cut}(\Gamma)$, which jointly terminates with the apex signal, i.e., $x_{cut}(\Gamma_a) = 0$. Most importantly, upon grating excitation (vertical line on the right), electrons are also detected up to values of $\Gamma = \Gamma_a$, although direct photoemission from the grating region is suppressed for $\Gamma \geq 0.7$, the value at which the cut-off position reaches the grating. We can therefore conclude that grating illumination results in electron emission from the apex, mediated by resonant SPP excitation.

Besides the selection of possible emission regions, it should be noted that Γ also has a pronounced effect on the trajectories of emitted electrons. In particular, for increasing Γ-values, the electrostatic field close to the apex acts as a focusing lens, which can be demonstrated by considering the spatial emission patterns for different conditions. Figures 3(c) and 3(d) display recorded images under grating excitation and for Γ values below (d) and near (c) the apex cut-off Γ_a (see arrows in Fig. 3(b)). In Fig. 3(d), two contributions are found, namely, an arc-shaped distribution of electrons directly emitted from the grating and a largely uniform distribution from apex electrons. Increasing Γ towards Γ_a reduces the radius of the arc feature until it vanishes (near $\Gamma = 0.7$). Upon approaching Γ_a, also the apex contribution is focused to a narrow spot (see Fig. 3(c)). The present setup is not able to quantitatively determine beam parameters such as brightness and emittance.[52] These quantities will be subject to investigation in the tip-based ultrafast transmission electron microscope we recently developed.[47] (The supplementary material[53] provides a movie of the spatial electron patterns for grating illumination, recorded as a function of Γ.) The focusing action of the suppressor additionally causes the lower edge of the diagonal stripe feature. Specifically, for a given emission position, a certain focusing and thus a threshold value of Γ is required to collect the electrons by the finite solid angle of detection. Below this threshold, electron paths are cropped by the MCP aperture. For completeness, in Fig. 3(b), we label those Γ values at which the two-dimensional scans in Figs. 2(b) and 2(c) are recorded.

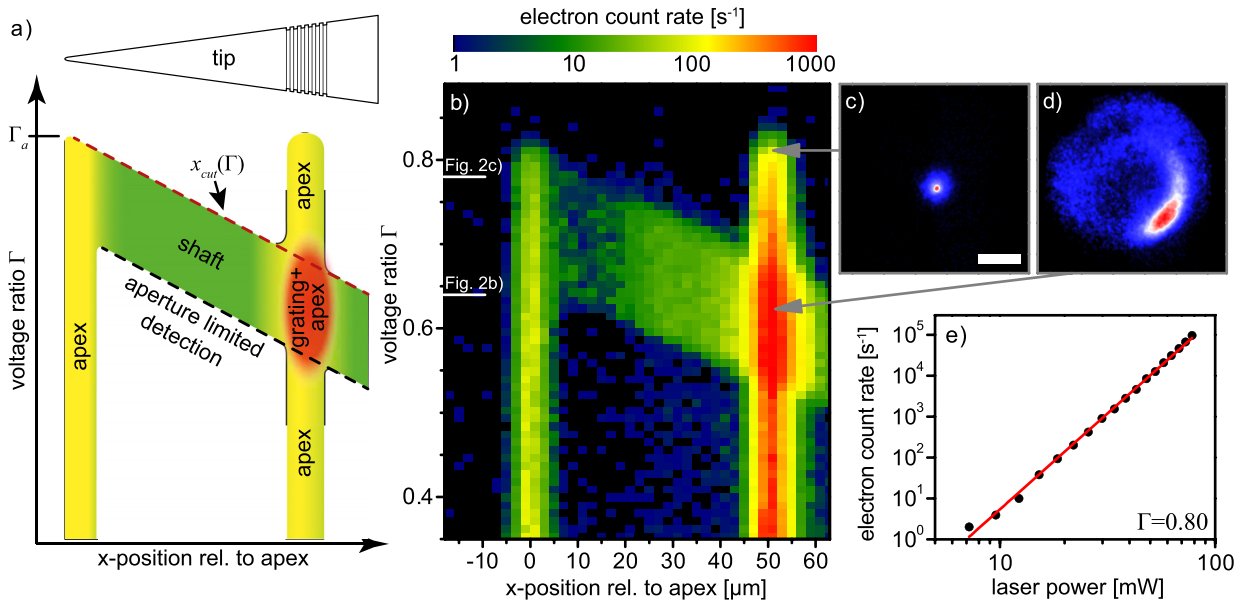

FIG. 3. (a) Schematic assignment of features in position- and Γ-dependent electron emission (see experimental data in (b)) to specific regions of emission. (b) Color-coded map of the electron count rate (logarithmic scale, integrated over detector area, and average laser power: 17 mW) as a function of Γ and focal spot position (scan line: cf. Fig. 2(c)). Vertical lines correspond to excitation on the apex ($x = 0$) and grating ($x = 50\ \mu$m). The Γ-dependent shift of the cut-off position on the shaft causes the diagonal stripe. Direct emission from positions to the right of the cut-off line (see $x_{cut}(\Gamma)$ in (a)) is suppressed. The observation of strong emission for grating excitation and at large Γ (up to apex suppression at Γ_a) thus demonstrates that these electrons are emitted at the apex. (c) Recorded electron image for $\Gamma \approx \Gamma_a$ exhibiting a focused spot (diameter 0.7 mm (full-width-half-maximum), scale bar: 5 mm). (d) For $0.55 < \Gamma < 0.7$, the pattern is composed of a largely uniform distribution from the apex, and shaft/grating electrons forming an arc-shape (bottom right). The electron images correspond to planes perpendicular to the tip axis. From this viewing direction, the grating is located on the right. (e) Nonlinear power-dependence of the electron current. Approximately 10^5 electrons/s are detected at an incident power of 78 mW. An effective nonlinearity of 4.7 (red line) is observed.

As photoemission currents from the tip end are generated for both direct apex illumination and grating illumination (currents denoted by J_{ap} and J_{gr}, respectively), it is interesting to consider the relative electron yields J_{gr}/J_{ap} for these two forms of excitation. In all our experiments, we obtained substantially higher emission upon grating excitation. At the conditions from Fig. 2, which were chosen to show both direct apex emission and grating-mediated emission, about 20 times more electrons from the apex are emitted upon grating illumination, similar to the recent results.[51] However, it should be noted that the specific focusing conditions, including wavefront tilt and curvature, strongly influence the mode overlap and thereby the specific relative emission yield. For optimized grating coupling, we achieved a ratio of $J_{gr}/J_{ap} = 150$. This enhancement clearly results from superior mode-matching between the far-field radiation and the extended grating,[54] as compared to direct apex excitation, and it may be used to estimate the resulting local intensities in both scenarios. To this end, we first have to determine the effective nonlinearity of the photoemission process. Figure 3(e) shows in a double-logarithmic plot the photocurrent from the apex as a function of laser power incident on the grating. A current of $J_{gr} \approx 10^5$ electrons/s is obtained for a power of $P = 78$ mW, and the current scales with an effective nonlinearity $n = 4.7$, i.e., $J_{gr} \propto P^n$ (solid red line), close to the expected value of 4. Thus, the field strength obtained at the apex for grating illumination exceeds that for direct illumination by a factor $(150)^{1/2n} \approx 1.7$ (a value of 1.32 was given in Ref. 51). Employing the emission current from the smooth shaft as a reference, field enhancement factors (defined as local apex field strength over incident field strength) for both excitation conditions can be estimated, and we find apex field enhancements of 6.4 and 3.8 for grating and direct illumination, respectively. In order to derive a normalized quantum efficiency of the nonlinear photoemission process from the measurements, we describe the total emitted charge as $Q = A\tau(s_n I)^n$, where A is the apex area, τ is the pulse duration at the apex (estimated to about 20 fs on the apex, influenced by some resonance narrowing[10] and minor SPP group-velocity dispersion[19,55]), I is the local intensity, and s_n is a coefficient containing the quantum efficiency of the multiphoton process at the measured effective nonlinearity n. Using this relation and the experimental parameters, we obtain a value of $s_n = 2.3 \times 10^{-15} \left(\frac{\mathrm{A}}{\mathrm{nm}^2}\right)^{1/n} \frac{\mathrm{cm}^2}{\mathrm{W}}$ for $n = 4.7$.[56]

In conclusion, we demonstrated site-sensitive multiphoton photoemission from a sharp gold nanotip equipped with a resonant grating structure. In the experiments, the tip was integrated into an extractor-suppressor-type gun assembly, which is fully compatible with existing transmission electron microscope geometries and allows for manipulating the electrostatic environment of the tip. In this way, a confinement of the photoemission to a very small apex region and a complete suppression of electron emission from the grating are achieved. Concerning future applications of the presented source concept in ultrafast electron microscopy and diffraction, this control over both the transversal beam properties and the local extraction fields will be highly beneficial, e.g., by electron beam collimation and by alleviating space charge problems from non-localized shaft emission. More generally, we believe that the photoemission induced by tailored plasmonic fields presents a powerful new degree of freedom to shape complex electronic wavefronts with well-defined linear and angular momentum distributions.

We gratefully acknowledge funding by the Deutsche Forschungsgemeinschaft (DFG) (SFB-1073, projects A5 & C4). We thank Karin Ahlborn for help in tip fabrication.

[1]W. L. Barnes, A. Dereux, and T. W. Ebbesen, Nature **424**, 824 (2003).
[2]S. A. Maier, *Plasmonics: Fundamentals and Applications*, 1st ed. (Springer, New York, 2007).
[3]J. A. Schuller, E. S. Barnard, W. Cai, Y. C. Jun, J. S. White, and M. L. Brongersma, Nat. Mater. **9**, 193 (2010).
[4]D. K. Gramotnev and S. I. Bozhevolnyi, Nat. Photonics **4**, 83 (2010).
[5]L. Novotny and N. van Hulst, Nat. Photonics **5**, 83 (2011).
[6]A. J. Babadjanyan, N. L. Margaryan, and K. Nerkararyan, J. Appl. Phys. **87**, 3785 (2000).
[7]M. Stockman, Phys. Rev. Lett. **93**, 137404 (2004).
[8]D. K. Gramotnev and S. I. Bozhevolnyi, Nat. Photonics **8**, 13 (2013).
[9]B. Schröder, T. Weber, S. V. Yalunin, T. Kiel, C. Matyssek, M. Sivis, S. Schäfer, F. von Cube, S. Irsen, K. Busch, C. Ropers, and S. Linden, Phys. Rev. B **92**, 085411 (2015).
[10]C. Ropers, C. C. Neacsu, T. Elsaesser, M. Albrecht, M. B. Raschke, and C. Lienau, Nano Lett. **7**, 2784 (2007).
[11]C. C. Neacsu, S. Berweger, R. L. Olmon, L. V. Saraf, C. Ropers, and M. B. Raschke, Nano Lett. **10**, 592 (2010).
[12]S. Berweger, J. M. Atkin, X. G. Xu, R. L. Olmon, and M. B. Raschke, Nano Lett. **11**, 4309 (2011).
[13]M. Esmann, S. F. Becker, B. B. da Cunha, J. H. Brauer, R. Vogelgesang, P. Groß, and C. Lienau, Beilstein J. Nanotechnol. **4**, 603 (2013).
[14]C. C. Neacsu, S. Berweger, and M. B. Raschke, NanoBiotechnology **3**, 172 (2007).
[15]S. Berweger, J. M. Atkin, R. L. Olmon, and M. B. Raschke, J. Phys. Chem. Lett. **1**, 3427 (2010).
[16]F. De Angelis, G. Das, P. Candeloro, M. Patrini, M. Galli, A. Bek, M. Lazzarino, I. Maksymov, C. Liberale, L. C. Andreani, and E. Di Fabrizio, Nat. Nanotechnol. **5**, 67 (2010).
[17]D. Sadiq, J. Shirdel, J. S. Lee, E. Selishcheva, N. Park, and C. Lienau, Nano Lett. **11**, 1609 (2011).
[18]S. Berweger, J. M. Atkin, R. L. Olmon, and M. B. Raschke, J. Phys. Chem. Lett. **3**, 945 (2012).
[19]S. Schmidt, B. Piglosiewicz, D. Sadiq, J. Shirdel, J. S. Lee, P. Vasa, N. Park, D.-S. Kim, and C. Lienau, ACS Nano **6**, 6040 (2012).
[20]A. Giugni, M. Allione, B. Torre, G. Das, M. Francardi, M. Moretti, M. Malerba, G. Perozziello, P. Candeloro, and E. Di Fabrizio, J. Opt. **16**, 114003 (2014).
[21]C. Ropers, D. R. Solli, C. P. Schulz, C. Lienau, and T. Elsaesser, Phys. Rev. Lett. **98**, 043907 (2007).
[22]B. Barwick, C. Corder, J. Strohaber, N. Chandler-Smith, C. Uiterwaal, and H. Batelaan, New J. Phys. **9**, 142 (2007).
[23]P. Hommelhoff, C. Kealhofer, and M. A. Kasevich, Phys. Rev. Lett. **97**, 247402 (2006).
[24]P. Hommelhoff, Y. Sortais, A. Aghajani-Talesh, and M. A. Kasevich, Phys. Rev. Lett. **96**, 077401 (2006).
[25]C. Ropers, T. Elsaesser, G. Cerullo, M. Zavelani-Rossi, and C. Lienau, New J. Phys. **9**, 397 (2007).
[26]H. Yanagisawa, C. Hafner, P. Doná, M. Klöckner, D. Leuenberger, T. Greber, M. Hengsberger, and J. Osterwalder, Phys. Rev. Lett. **103**, 257603 (2009).
[27]H. Yanagisawa, C. Hafner, P. Doná, M. Klöckner, D. Leuenberger, T. Greber, J. Osterwalder, and M. Hengsberger, Phys. Rev. B **81**, 115429 (2010).
[28]M. Schenk, M. Krüger, and P. Hommelhoff, Phys. Rev. Lett. **105**, 257601 (2010).
[29]R. Bormann, M. Gulde, A. Weismann, S. V. Yalunin, and C. Ropers, Phys. Rev. Lett. **105**, 147601 (2010).
[30]M. Krüger, M. Schenk, P. Hommelhoff, and M. Kruger, Nature **475**, 78 (2011).
[31]D. J. Park, B. Piglosiewicz, S. Schmidt, H. Kollmann, M. Mascheck, and C. Lienau, Phys. Rev. Lett. **109**, 244803 (2012).
[32]G. Herink, D. R. Solli, M. Gulde, and C. Ropers, Nature **483**, 190 (2012).

[33]L. Wimmer, G. Herink, D. R. Solli, S. V. Yalunin, K. E. Echternkamp, and C. Ropers, Nat. Phys. **10**, 432 (2014).
[34]H. Yanagisawa, M. Hengsberger, D. Leuenberger, M. Klöckner, C. Hafner, T. Greber, and J. Osterwalder, Phys. Rev. Lett. **107**, 087601 (2011).
[35]A. R. Bainbridge and W. A. Bryan, New J. Phys. **16**, 103031 (2014).
[36]R. J. D. Miller, Annu. Rev. Phys. Chem. **65**, 583 (2014).
[37]D. J. Flannigan and A. H. Zewail, Acc. Chem. Res. **45**, 1828 (2012).
[38]J. S. Kim, T. LaGrange, B. W. Reed, M. L. Taheri, M. R. Armstrong, W. E. King, N. D. Browning, and G. H. Campbell, Science **321**, 1472 (2008).
[39]A. Hanisch-Blicharski, A. Janzen, B. Krenzer, S. Wall, F. Klasing, A. Kalus, T. Frigge, M. Kammler, and M. Horn-von Hoegen, Ultramicroscopy **127**, 2 (2013).
[40]M. Eichberger, H. Schäfer, M. Krumova, M. Beyer, J. Demsar, H. Berger, G. Moriena, G. Sciaini, and R. J. D. Miller, Nature **468**, 799 (2010).
[41]L. Piazza, D. Masiel, T. LaGrange, B. Reed, B. Barwick, and F. Carbone, Chem. Phys. **423**, 79 (2013).
[42]V. R. Morrison, R. P. Chatelain, K. L. Tiwari, A. Hendaoui, A. Bruhacs, M. Chaker, and B. J. Siwick, Science **346**, 445 (2014).
[43]S. Lahme, C. Kealhofer, F. Krausz, and P. Baum, Struct. Dyn. **1**, 034303 (2014).
[44]C. Gerbig, A. Senftleben, S. Morgenstern, C. Sarpe, and T. Baumert, New J. Phys. **17**, 043050 (2015).
[45]A. Paarmann, M. Gulde, M. Muller, S. Schafer, S. Schweda, M. Maiti, C. Xu, T. Hohage, F. Schenk, C. Ropers, and R. Ernstorfer, J. Appl. Phys. **112**, 113109 (2012).
[46]J. Hoffrogge, J. Paul Stein, M. Krüger, M. Förster, J. Hammer, D. Ehberger, P. Baum, and P. Hommelhoff, J. Appl. Phys. **115**, 094506 (2014).
[47]A. Feist, K. E. Echternkamp, J. Schauss, S. V. Yalunin, S. Schäfer, and C. Ropers, Nature **521**, 200 (2015).
[48]M. Gulde, S. Schweda, G. Storeck, M. Maiti, H. K. Yu, A. M. Wodtke, S. Schäfer, and C. Ropers, Science **345**, 200 (2014).
[49]E. Quinonez, J. Handali, and B. Barwick, Rev. Sci. Instrum. **84**, 103710 (2013).
[50]M. Müller, A. Paarmann, and R. Ernstorfer, Nat. Commun. **5**, 5292 (2014).
[51]J. Vogelsang, J. Robin, B. J. Nagy, P. Dombi, D. Rosenkranz, M. Schiek, P. Groß, and C. Lienau, Nano Lett. **15**, 4685 (2015).
[52]R. Bormann, S. Strauch, S. Schäfer, and C. Ropers, J. Appl. Phys. **118**, 173105 (2015).
[53]See supplementary material at http://dx.doi.org/10.1063/1.4937121 for a movie of the electron distributions upon grating illumination, recorded as a function of Γ.
[54]S. Schmidt, P. Engelke, B. Piglosiewicz, M. Esmann, F. Simon, K. Yoo, N. Park, C. Lienau, and P. Groß, Opt. Express **21**, 26564 (2013).
[55]V. Kravtsov, J. M. Atkin, and M. B. Raschke, Opt. Letters **38**, 1322 (2013).
[56]We obtain similar values of $s_n = 2.7 \times 10^{-15} \left(\frac{\mathrm{A}}{\mathrm{nm}^2}\right)^{1/n} \frac{\mathrm{cm}^2}{\mathrm{W}}$ with n = 4.5 and $s_n = 2.8 \times 10^{-15} \left(\frac{\mathrm{A}}{\mathrm{nm}^2}\right)^{1/n} \frac{\mathrm{cm}^2}{\mathrm{W}}$ with n = 5 for the data reported in Refs. 51 and 29, respectively, although this may not be expected for Ref. 51 given the very different photon energies used.